ADVANCED FUNCTIONAL MATERIALS
www.afm-journal.de

Check for updates

Electron Trap Dynamics in Polymer Light-Emitting Diodes

*Matthias Diethelm, Michael Bauer, Wei-Hsu Hu, Camilla Vael, Sandra Jenatsch, Paul W. M. Blom, Frank Nüesch, and Roland Hany**

Semiconducting polymers are being studied intensively for optoelectronic device applications, including solution-processed light-emitting diodes (PLEDs). Charge traps in polymers limit the charge transport and thus the PLED efficiency. It is firmly established that electron transport is hindered by the presence of the universal electron trap density, whereas hole trap formation governs the long-term degradation of PLEDs. Here, the response of PLEDs to electrical driving and breaks covering the timescale from microseconds to (a few) hours is studied, thus focusing on electron traps. As reference polymer, a phenyl-substituted poly(*para*-phenylene vinylene) (PPV) copolymer termed super yellow (SY) is used. Three different traps with depths between ≈0.4 and 0.7 eV, and a total trap site density of ≈2 × 10^{17} cm^{-3} are identified. Surprisingly, filling of deep traps takes minutes to hours, at odds with the common notion that charge trapping is complete after a few hundred microseconds. The slow trap filling feature for PLEDs is confirmed using poly(2-methoxy-5-(2-ethylhexyloxy)-1,4-phenylene vinylene (MEH-PPV) and poly(3-hexylthiophene) (P3HT) as active materials. This unusual phenomenon is explained with trap deactivation upon detrapping and slow trap reactivation. The results provide useful insight to pinpoint the chemical nature of the universal electron traps in semiconducting polymers.

1. Introduction

Polymer light-emitting diodes (PLEDs) are attractive electroluminescence devices for large-area display and lighting applications.[1,2] The presence of traps for electrons and holes in conjugated polymers, however, seriously limits the device efficiency and lifetime. It has been shown that there exists a universal electron trap site density, with a number of traps of 1–3 × 10^{17} cm^{-3}, centered at an energy of ≈3.6 eV below the vacuum level.[2–6] This electron trap distribution is identical for a wide range of polymers considered.[3] This indicates that these electron traps have a common (extrinsic) origin, and excludes intrinsic defects (such as kinks in the polymer backbone) or impurities from the synthesis that are material-specific. As possible origin, water–oxygen complexes were identified as a cause for trapping.[3,4] For PPV polymers, the trap energy translates into a trap depth in the range of E_t = 0.6–0.7 eV.[2,4,5] Electron traps are not limited to conjugated polymers, but also occur in vacuum-deposited small-molecular semiconductors.[6] They decrease the electron mobility and light emission via nonradiative recombination with free holes. In addition, while operating PLEDs at constant current over many tens of hours, the voltage continuously increases and the luminance decreases.[1] This is due to the formation of hole traps via the interaction of excitons with free holes. Hole traps grow over orders of magnitude with time and dictate the long-term stability of PLEDs.[1,5,7,8] It has been predicted[9] and experimentally confirmed[1,10] that by diluting the polymer with an insulating matrix, the effect of traps can be effectively eliminated, resulting in long-term stable PLEDs with a luminance efficacy (cd A^{-1}) that increases by almost a factor of 2.

Here, we study the response of super yellow (SY) PLEDs[1,11,12] to electrical stress pulses and breaks covering a time range of eight orders of magnitude. The chemical structure of SY is shown in Figure S1 (Supporting Information). We identify first a fraction of shallow electron traps with a trap depth of ≈0.4 eV. These traps are permanently present in the polymer with a density in the range of 1 × 10^{17} cm^{-3}, and trapping takes ≈200 µs. Trapping is a downhill process in energy, and is therefore expected to be fast. We show that a timescale of 100 µs for charge trapping also follows from the corresponding electron trap density equation.

M. Diethelm, M. Bauer, W.-H. Hu, F. Nüesch, R. Hany
Empa
Swiss Federal Laboratories for Materials Science and Technology
Laboratory for Functional Polymers
8600 Dübendorf, Switzerland
E-mail: roland.hany@empa.ch

M. Diethelm, W.-H. Hu, C. Vael, F. Nüesch
EPFL
Institute of Materials Science and Engineering
Ecole Polytechnique Fédérale de Lausanne, Station 12, Lausanne 1015, Switzerland

C. Vael, S. Jenatsch
Fluxim AG
Katharina-Sulzer-Platz 2, Winterthur 8400, Switzerland

P. W. M. Blom
Max Planck Institute for Polymer Research
Ackermannweg 10, 55128 Mainz, Germany

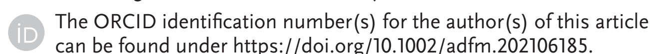
The ORCID identification number(s) for the author(s) of this article can be found under https://doi.org/10.1002/adfm.202106185.

© 2022 The Authors. Advanced Functional Materials published by Wiley-VCH GmbH. This is an open access article under the terms of the Creative Commons Attribution License, which permits use, distribution and reproduction in any medium, provided the original work is properly cited.

DOI: 10.1002/adfm.202106185

© 2022 The Authors. Advanced Functional Materials published by Wiley-VCH GmbH

Further, we identify electron traps with trap depths of ≈0.5 and 0.7 eV with a total concentration in the same range of 1×10^{17} cm^{-3}. By virtue of the trap depth and concentration, we assign these traps to the universal electron traps present in these materials. Deep traps detrap slowly after switching off, as expected. Surprisingly, however, the filling of these traps is also very slow, as we infer from device recovery trends after rest that proceed over many minutes. We explain this finding with that the universal electron trap species effectively deactivate when the trap empties, either by thermal emission or after light excitation. Subsequently after switch-on, the probability that a deactivated trap species traps a passing charge is low, explaining the long trap filling time observed. The scenario of trap deactivation upon detrapping provides important information on the chemical nature of the universal electron traps in semiconducting polymers. Specifically, we discuss that slow trap filling is consistent with a diffusion process between oxygen and water precursor trap species that form a stable trapped complex only while meeting, but that the neutral complex after detrapping is weakly bound and water and oxygen separate via diffusion.

2. Results

The cycle for electron traps when a PLED is switched on to drive and then back to rest can be readily understood. In a device at rest, electron traps are empty. When, for example, a voltage bias is applied, the initial flow of mobile electron charge increases, as well as the radiative Langevin recombination between mobile electrons and holes. Over time, electron traps fill up and immobile charge replaces mobile charge. This results in a decrease in the current that is proportional to the number of filled traps. At the same time, nonradiative Shockley–Read–Hall (SRH) recombination between trapped electrons and free holes increases, thereby reducing the Langevin recombination. When the bias is switched off, free holes and electrons recombine rapidly. Subsequently, trapped electrons detrap via thermal emission, and the detrapping time is a measure of the trap depth. Thus, by measuring the current and light emission decay after switch-on and the detrapping time after switch-off, we obtain information about the trap filling time and the trap concentration, as well as the trap depth. Similar considerations apply when driving a device at a constant current bias. The situation can be quantified with electrical and optical numerical simulations.

2.1. Electron Trap Dynamics at Short Timescales

First, we applied a voltage pulse to a pristine PLED and measured the current and light response at short timescales (**Figure 1**a). The current peak before ≈2 µs is a displacement current due to the fast change of the electric field when the voltage bias is switched on within a few microseconds. In the measurement, the displacement current overlaps to some extent with a current peak at early times. Figure 1b,c shows simulations of the light and current transients. Simulation reproduces the displacement current qualitatively and identifies the current peak. The light peak at 20 µs and the initial current decline are due to the electron trap filling, in an unaged device the hole trap site density is very low.[1] First, filled electron traps result in a trap space charge that displaces space charge from free charges (curve "electron density" in Figure 1c). This displacement happens because the electric field remains nearly constant during trap filling, which means the total space charge, coupled to the field by the Poisson equation, remains constant as well. Trapped charges do not contribute to the current in the device; thus, the current and the emitted light decrease. Second, SRH recombination increases with more trapped charge, reducing the emissive Langevin recombination. This explains why the decrease of light emission is stronger than the decrease of the current.

The transients in Figure 1a reach a steady state after ≈200 µs, but after ≈1 ms both the current and light slowly start to decline; we discuss this effect further below. For the simulation, the electron trap site density was set to 1×10^{17} cm^{-3} and the resulting trap filling time constant was 40 µs, other simulation parameters are summarized in Supporting Information Note S1. The transient device response confirms the received opinion that charge trapping is a fast process. Also, the recombination between free electrons and holes takes place rapidly, and when the device is switched off the electroluminescence signal decays within <1 µs (Figure S1, Supporting Information).

To rationalize the fast electron trap filling, we consider the trap density equation in the on state. The time dependence of the trapped electrons $\frac{dn_t}{dt}$ is given by the competition between trap filling and detrapping processes, including emission and recombination. In Equation (1), $R_{fill} = C_n * n(N_t - n_t)$, with the free electron density n that gets trapped with an electron capture coefficient C_n by the remaining free electron trap sites $(N_t - n_t)$. N_t is the trap site density and n_t the trapped electron density. The SRH recombination is $R_{SRH} = C_p * p * n_t$, with the free hole density p recombining with the trapped electron density n_t with a hole capture coefficient C_p. In addition, the term $e_n * n_t$ for the emission of trapped electrons back to the conduction band is added.

$$\frac{dn_t}{dt} = C_n \times n(N_t - n_t) - e_n \times n_t - C_p \times p \times n_t \tag{1}$$

With the condition that at switch-on the electron traps are empty $(n_t(0) = 0)$, the solution of Equation (1) is

$$n_t(t) = \frac{a}{b} \times \left(1 - e^{-b \times t}\right) \tag{2}$$

with $a = C_n \times n \times N_t$ and $b = C_n \times n + e_n + C_p \times p$.

The steady-state situation at $t \to \infty$ is given by

$$n_t = \frac{C_n n \times N_t}{C_n n + e_n + C_p p} \to \frac{n_t}{N_t} = \frac{C_n n}{C_n n + e_n + C_p p} \tag{3}$$

and in equilibrium the ratio n_t/N_t of trapped electrons to trapping sites depends on the term $\frac{C_n n}{C_n n + e_n + C_p p}$. Assuming $e_n = 0$ (deep traps), the final trap density depends only on the terms $C_p p$ from SRH recombination and $C_n n$ from trap filling. In the case $C_n n = C_p p$, Equation (3) becomes $\frac{n_t}{N_t} = \frac{1}{2}$, which means half of the traps are filled in equilibrium. If $C_n n \gg C_p p$, $\frac{n_t}{N_t} = 1$, since all traps will finally be filled. On the other hand,

© 2022 The Authors. Advanced Functional Materials published by Wiley-VCH GmbH

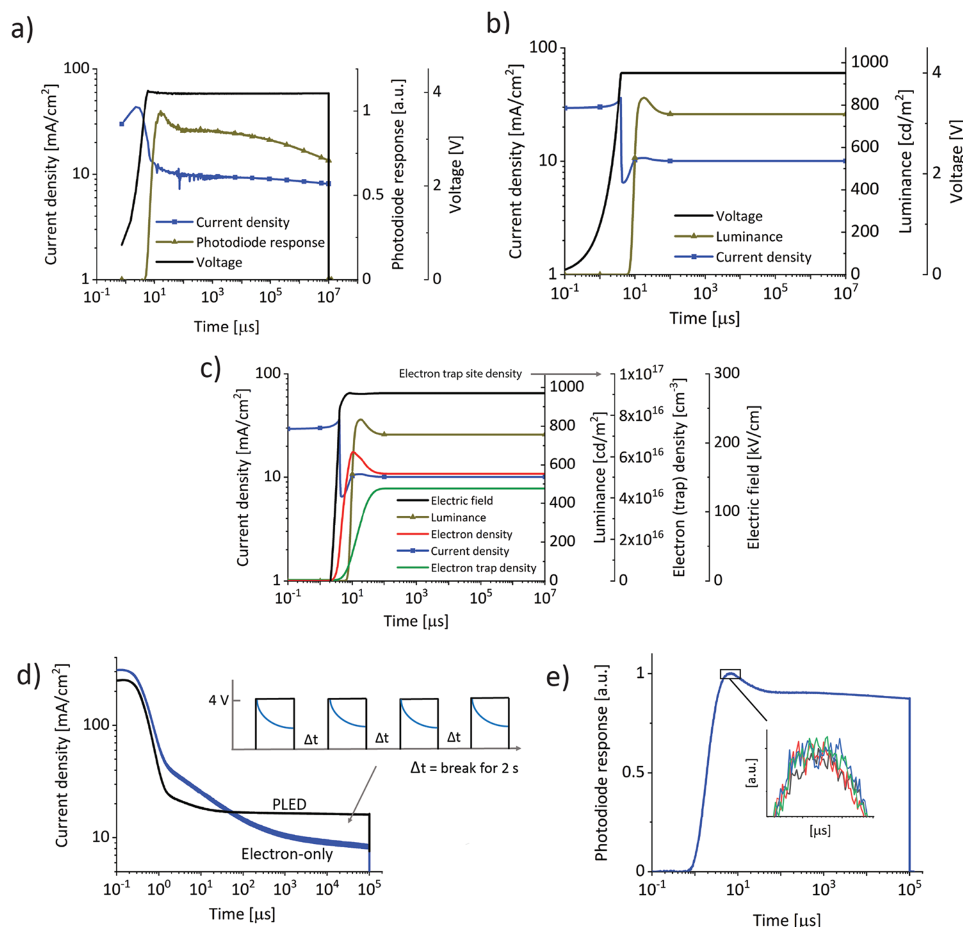

Figure 1. Transient response of pristine SY PLEDs at short timescales. a) Current and light transients measured when a voltage pulse is applied for 10 s. b) Transient drift-diffusion simulation with c) the corresponding simulated charge densities during the voltage pulse. A sequence of four short (0.1 s) voltage pulses with a break time of 2 s in between is applied to a pristine PLED and a pristine electron-only device, d) displays the current and e) the light measured during the pulses.

$C_n n \ll C_p p$ leads to $\frac{n_t}{N_t} = 0$ because a very strong SRH recombination empties a trap instantly after filling.

We evaluate the time until equilibrium. At $= \frac{1}{b}$, $n(t) = \frac{a}{b}\left(1 - e^{-1}\right) = 0.63 \times \frac{a}{b}$, which means that 63% of the traps of the steady-state ratio are already filled. It shows that the fastest process dominates the time constant. Capture coefficients are in the range of $10^{-12} - 10^{-14}$ cm^3 s^{-1}.[1,2] For a capture coefficient 5×10^{-13} cm^3 s^{-1} and a free electron density of 5×10^{16} cm^{-3} as in the simulation, the time constant $\frac{1}{C_n \times n}$ is 40 µs, and even smaller if the other processes (e_n, $C_p p$) are considered as well.

We applied a sequence of voltage pulses and rest periods to a pristine PLED and an electron-only device and measured the current and light response (Figure 1d,e). The four current and light transients almost perfectly overlap (insert of Figure 1e). From this we conclude that complete electron detrapping occurs during a break of 2 s; if there were trapped electrons still present after the break time, the current and light during a subsequent voltage pulse would start at a lower level. From a quantitative analysis (**Figure 2**e, see below) we find that detrapping related effects become visible after ≈650 µs and traps fully detrap within 100 ms.

From this time range, we can estimate the trap depth. When the bias is switched off, the free hole density p gets many orders of magnitude smaller at 0 V and SRH recombination is negligible. The same is true for the free electron density n, and Equation (1) simplifies to

$$\frac{dn_t}{dt} = -e_n * n_t \tag{4}$$

In this case, traps empty with the rate e_n,[13] which depends on $C_n (= 5 \times 10^{-13}$ cm^3 s^{-1}), the density of free electron states $N_{0,N}$ and the trap depth

$$e_n = C_n \times N_{0,N} \times \exp\left(\frac{E_t - LUMO}{kT}\right) \tag{5}$$

E_t is the trap energy, $LUMO$ the lowest unoccupied molecular orbital, and $N_{0,N} = 1 * 10^{27}\ m^{-3}$, which is a result of one state per cubic nanometer.[2] The measured times for the onset (≈650 µs) and completion (100 ms) of electron detrapping indicate

© 2022 The Authors. Advanced Functional Materials published by Wiley-VCH GmbH

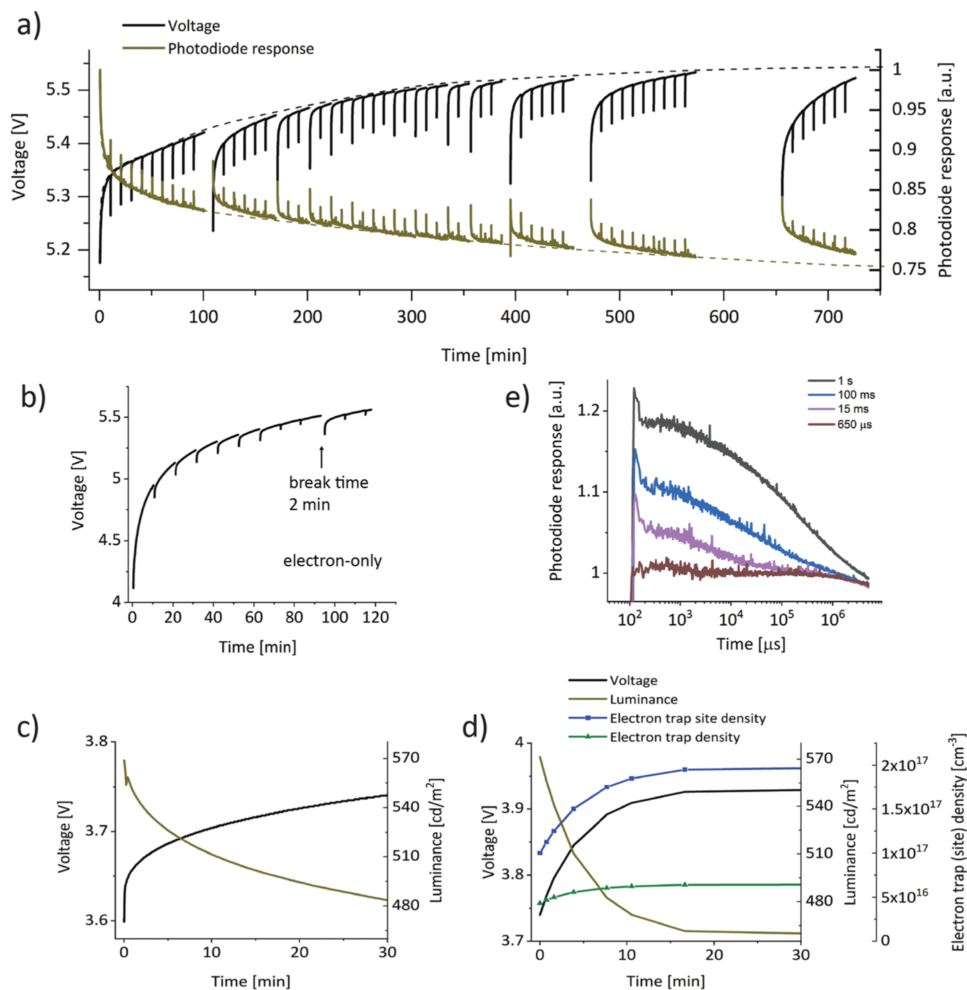

Figure 2. The slow electron trap dynamics in SY PLEDs. a) Voltage and light emission trend of a constant current-driven PLED (7.7 mA cm^{-2}). The current stress was interrupted at particular moments and the device rested at short-circuit (0 V) for a certain time before switching to bias again. b) Voltage trend of a constant current-driven electron-only device. c) Experimental and d) simulated voltage and luminance trend at a constant current of 7.7 mA cm^{-2} during the first 30 min. e) The break time between two 5 s long voltage pulses (4 V) was varied from 10 µs to 1 s and light transients were measured during the second voltage pulse.

a trap depth of $(E_t - LUMO) \approx 0.4$ eV, which leads to a time constant of $\frac{1}{e_n} = 10\,ms$ according to Equation (5). With that, $n_t\,(650\,\mu s) = N_0\ e^{-\frac{650\,\mu s}{10\,ms}} = 0.94 \times N_0$, i.e., detrapping has just started, and $n_t\,(100\,ms) = N_0\ e^{-\frac{100\,ms}{10\,ms}} = 5 \times 10^{-5} \times N_0$, which means trapped electrons have de-trapped completely. Changing the trap depth by only 0.05 eV results in a time constant shift by a factor of 10, such that the resulting detrapping dynamics does not agree with the established time range. For a trap depth of 0.45 eV, there are still 40% of the traps present after 100 ms, and for 0.35 eV already 8% of the traps have detrapped after 80 µs, where we do not see any effect in the measurement.

Summarizing so far, we identify in SY a shallow electron trap with a trap depth of ≈0.4 eV and a trap site density of $\approx 1 \times 10^{17}$ cm^{-3}. These traps are present in the pristine material already, charge trapping takes around 200 µs, and de-trapping is completed after ≈100 ms.

2.2. The Slow Electron Trap Dynamics

We turn our attention to the observation from Figure 1a that after ≈1 ms both the current and light slowly start to decline. Figure 2a shows the voltage and luminance trend of a SY PLED driven at a constant current bias of 7.7 mA cm^{-2} for 12 h, interrupted by breaks at specific moments. To check the consistent device response over the long measurement time, the current was interrupted after every 10 min for a short duration of 3.5 s. During some breaks, the device was rested at short-circuit for longer times, ranging from 3 s (limited by the experimental setup) to 1.5 h. After every break, an intermediate increase in device performance is observed, both electrically (apparent via a decrease of the starting voltage) and optically (apparent via an increased starting photodiode response). Subsequently, the voltage and photodiode recover slowly back to the trend line before the break. This measurement protocol did not change the long-term behavior of the PLED, as indicated by the dashed curve. The steady increase of voltage and decrease of

© 2022 The Authors. Advanced Functional Materials published by Wiley-VCH GmbH

light emission over many hours is attributed to the continuous formation of hole traps, in agreement with literature.[1] Data in Figure 2a were measured on a device with SY coated from THF, we observed similar long-term transients for devices coated from toluene (Note S2, Supporting Information).

In a few cases, similar transients were reported for organic light-emitting diodes that continued for seconds to hours. This topic received little attention so far, and the effects were, suggestively, explained with temperature variations, reorientation of internal dipoles as well as redistribution of ionic impurities or trapped charge.[14–21] In the Supporting Information Note S2 we consider – and carefully exclude – that these effects explain the observed recovery trend in our case.

We explain the observation by the presence of deep electron traps that detrap slowly at rest and at switch-on both the electrical and optical performance are improved until the traps fill up again. The fact that the voltage and light recovery takes a long time, however, is an unexpected observation, clearly in contrast to the general notion that trap filling occurs on a timescale of a few 100 µs or less, irrespective of the depth of the trap level. We ascribe the slow recovery transients to the fact that detrapping effectively deactivates the trap, followed by slow trap reactivation. In the following, we designate this phenomenon "trap deactivation."

We evaluate the magnitude of the relaxed voltage (undershoot) and photodiode response (overshoot) as well as the recovery times to the steady state situation, which is the point where the measurement curve approaches the long-term transient, indicated by the dashed line. The trend is the same for all four quantities: the longer the break time, the larger is the voltage undershoot and recovery time, as well as the photodiode response overshoot and recovery time. The trends are summarized in Figure S2 (Supporting Information), which show logarithmic behavior with break time.

Three main observations emerge from these break experiments: i) The recovery time is in the range from minutes to hours. ii) The effect does not change over a drive time of 12 h, i.e., the same break duration at different points in time leads to similar light overshoots and voltage undershoots. iii) The initial increase of voltage and drop of photodiode response for a pristine device resembles the recovery after a break time of ≈1000 s at a later time. Statements (ii) and (iii) indicate that the relaxation and recovery process does not involve the hole traps, because they form continuously and grow in number over time. We applied the measurement sequence from Figure 2a to an electron-only device (Figure 2b) and observed the same general trend, as expected when electron traps dictate the proceedings. Trap deactivation is slower for the electron-only device, which can be explained with the absence of hole traps that activate a small deactivation channel via electron–hole trap–trap recombination (Figure S3, Supporting Information).

An assumed energetic trap depth of ≈0.7 eV results in a detrapping time constant at rest of 1000 s (Equation (5)), in good agreement with the measured relaxation timescale. We simulated the experimental voltage and luminance trend for a constant current-driven device over the first 30 min. Results in Figure 2d show that an electron trap site density of 1×10^{17} cm^{-3} develops over time, starting from a value of 1×10^{17} cm^{-3} at time zero that originates from the existing shallow traps that are filled immediately (Figure 1).

We repeated the experiment from Figure 2a with PLEDs using P3HT and MEH-PPV as an active material (**Figure 3**). In agreement with the observations made for SY PLEDs, we find that the decrease of the starting voltage correlates with the lengthening of the break time, which is explained by proceeding detrapping of deep electron traps at rest. We also observe that at switch-on the voltage recovers very slowly back to the trend line before the break, which we ascribe to trap deactivation upon detrapping. MEH-PPV differs by the side chains but is structurally related to SY, P3HT belongs to a different polymer family. It thus appears that the slow trap filling feature (and the underlying origin) is not restricted to SY, but applies to a broad range of semiconducting polymers.

For SY PLEDs, we studied the device response for break times <3 s. Therefore, we applied a sequence of two 5 s long voltage pulses to a pristine PLED. Pulses were separated by a variable break time (10 µs–1 s) and the device response was measured during the second voltage pulse with a high time resolution. Figure 2e displays the light transients for that measurement sequence. A light peak during the first 200 µs of the measurement time gets noticeable for break times above ≈650 µs; by comparing with data shown in Figure 1a, we

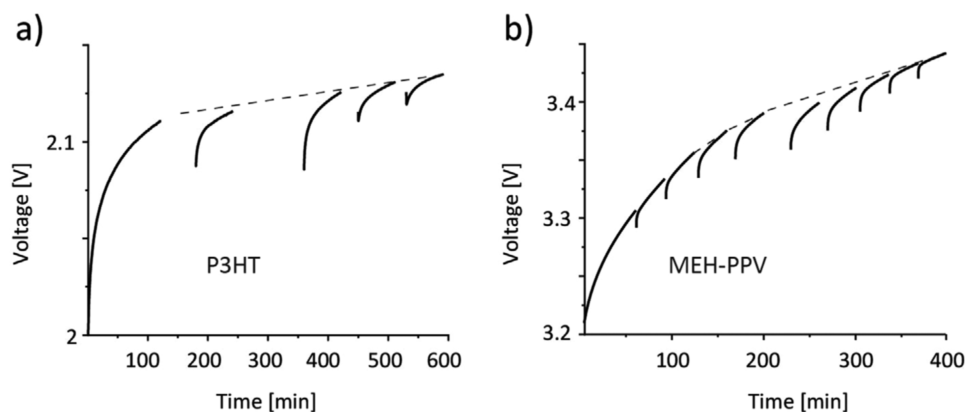

Figure 3. Voltage trends for a constant current-driven a) P3HT and b) MEH-PPV PLED (7.7 mA cm^{-2}). The current stress was interrupted at particular moments and the device rested for a certain time before switching to bias again.

© 2022 The Authors. Advanced Functional Materials published by Wiley-VCH GmbH

ascribe this feature to the filling of the shallow electron traps that empty during the break time. Complete detrapping of the shallow electron traps takes ≈100 ms because the magnitude of the short-term peak stays constant for longer break times. From the current transients for that measurement sequence we derive the same conclusion as discussed here for the light transients (Figure S2, Supporting Information).

It is interesting to note that data in Figure 2e clearly show that after a measurement time of ≈200 µs a second dynamic feature evolves. The photodiode response level increases with increasing break time and relaxes over the measurement time of 5 s back to the steady state value. Again, we ascribe this trend to a trap filling process of traps that empty during the break. A detrapping time of 1 s implies that the trap depth is close to 0.5 eV, clearly different from the shallow (0.4 eV) and deep (0.7 eV) trap levels we identified so far. We denote this trap as "intermediate." Both deep and intermediate traps share the common unusual feature that for a given detrapping period at rest the recovery time is much longer. We explain this phenomenon with trap deactivation.

Again, we estimate the intermediate trap site density from simulation and for this note that the photodiode trends between 1 ms and 1 s from Figures 1a and 2e closely match. In the simulation, we start from the steady-state situation in Figure 1b after 200 µs and add trap sites over time. For each portion, we simulate the resulting steady state luminance. An added intermediate trap site density of 3×10^{16} cm^{-3} results in a simulated decrease of the photodiode response between 1 ms and 1 s of 12%, in agreement with the experiment.

The simulated trap site density from Figure 2d (1×10^{17} cm^{-3}) represents the total of the intermediate and deep traps. With the intermediate trap site density (3×10^{16} cm^{-3}) at hand, we thus find that the concentration of deep traps is slightly higher, on the order of 7×10^{16} cm^{-3}.

2.3. Electron De-Trapping by Light

We obtain further evidence for trap deactivation from illumination experiments. Therefore, devices were rested at short-circuit and then a constant voltage was applied (**Figure 4**). Again, the initial device performance improved and a current overshoot occurred that recovered to the steady-state value. During the recovery time, we applied light pulses with a wavelength below the bandgap of SY. The first light pulse was applied directly at switch-on of the voltage, the second pulse during current recovery. From Figure 4 it can be seen that the current increases slowly during the duration of the second light pulse and recovers afterward.

The overall current decrease during the voltage pulse is due to the regeneration of intermediate and deep electron traps that deactivated at rest—at switch-on, the permanently present shallow traps fill up immediately and the current adjusts within 200 µs. Consequently, when light excites and empties a shallow trap, the trap fills up on the same fast timescale. Interestingly, during the second light pulse, the device response is much slower and it takes several tens of seconds until a new steady state is reached. We interpret this observation by that detrapping induced by light immediately deactivates the intermediate and deep traps, followed by slow reactivation over time. Slow trap site activation competes with trap site deactivation, and a new steady state adjusts during the light pulse. If light-induced detrapping would not result in trap deactivation, trap filling of deep traps would also occur within hundreds of microseconds, just like for the shallow traps, and the new steady state would adjust instantaneously on the timescale of the measurement. The timescale for the light experiment is the same as trap deactivation measured for breaks at short-circuit, supporting that detrapping by light deactivates the trap.

Similar transients as shown in Figure 4 were observed for irradiation wavelengths ranging from 740 to 1020 nm (Note S3, Supporting Information). We used the same photon flux at each wavelength, indicating that the trap absorption profile is rather flat between ≈650 and 1000 nm.

3. Discussion

By measuring the electrical and optical response of SY PLEDs to stress and rest periods ranging from microseconds to hours, we identify three electron trap levels and summarize the

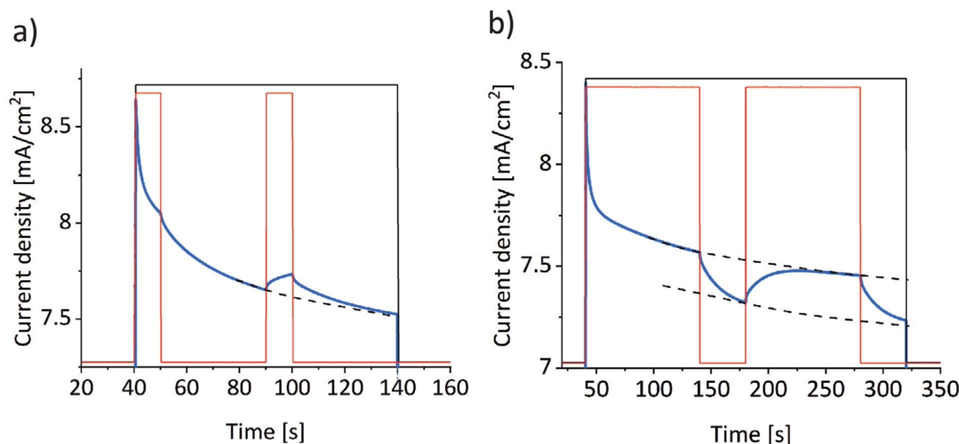

Figure 4. Electron detrapping by light. A constant voltage of 5.3 V (black) was applied to a SY PLED after a break time of 40 s. At voltage switch-on, the current (blue) overshoots and recovers over time to the steady state value. In (a), two LED pulses (red) with a wavelength of 656 nm were applied for 10 s during the measurement. In (b), the LED pulses had a length of 100 s.

© 2022 The Authors. Advanced Functional Materials published by Wiley-VCH GmbH

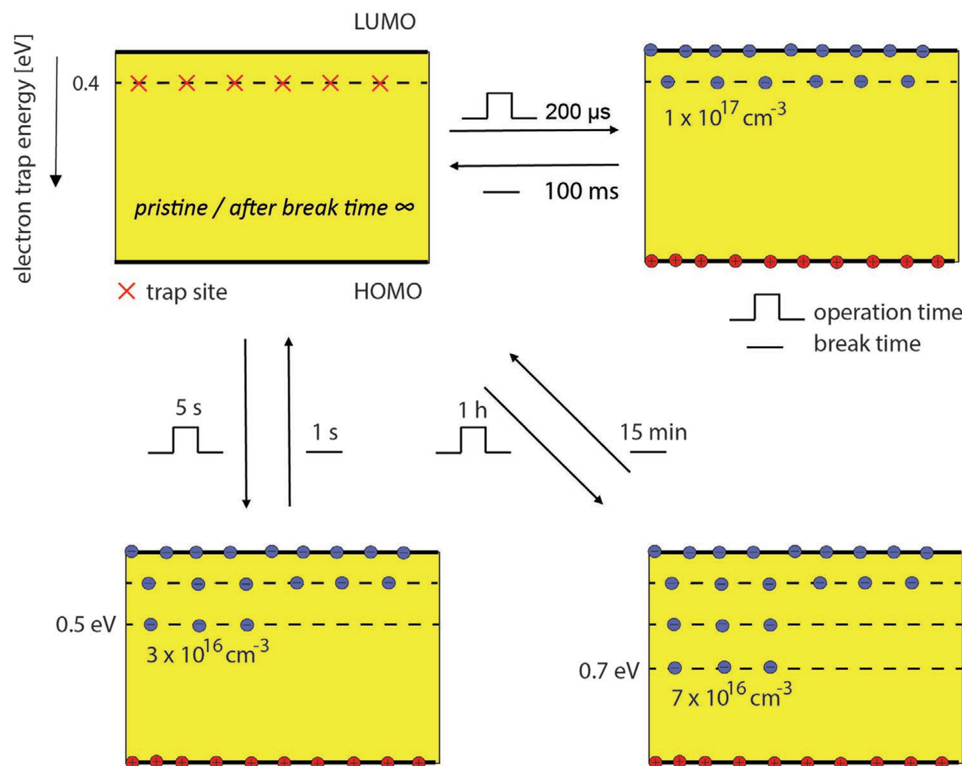

Figure 5. Schematic diagram summarizing the electron trap dynamics in SY PLEDs. Note that in the pristine device there are no (empty) trap sites present at trap levels of 0.5 and 0.7 eV, these traps deactivate upon detrapping. Indicated times are experimental values for which we observe complete trapping and device relaxation. Electron trap concentrations were evaluated via numerical simulation.

evaluated trap dynamics, energies of the trap levels and trap concentrations in **Figure 5**.

We define the trap depth with respect to the energy barrier a trapped electron has to overcome. In the picture of a Gaussian density of states (DOS) for the LUMO,[2,3,22] this energy barrier is best described by the difference between the trap level and the energy level $E_0 - E_a$, which is formally equivalent to the conduction-band edge, with the center of the Gaussian DOS E_0 minus the characteristic energy $E_a = \frac{\sigma^2}{2kT}$. E_a is ≈0.2 eV for a typical variance σ = 0.1 eV of the Gaussian DOS.[2] For the calculation of the trap depths we considered only detrapping by thermal emission and neglected hole trap formation during the first minutes of operation,[1] which opens presumably a small deactivation channel via electron–hole trap-trap recombination. Therefore, trap depths for intermediate and deep traps are actually slightly deeper than 0.5 and 0.7 eV. By virtue of the trap energies and their total concentration of ≈1 × 10^{17} cm^{-3}, we identify these traps with the universal electron trap site density present in these materials.[3] The detrimental effect of the developing electron traps on the device performance is substantial, and from the decaying luminance and increasing voltage trends shown in Figure 2c, it follows that the power conversion efficacy (lm W^{-1}) decreases by almost 20% over the first 30 min of operation (assuming the device is a Lambertian emitter).

The origin of charge trapping in organic semiconductor materials is presently not well understood, primarily because of the small trap concentrations involved, which makes the chemical nature of traps difficult to characterize. It remains to be seen whether the shallow electron traps are specific to SY or whether they can be identified in other semiconducting (PPV) polymers as well. These traps behave "normally" in the sense that trap filling is a fast process and is completed within ≈200 µs, as expected from the general notion of charge trapping in organic semiconducting materials. Two types of electron traps in PLEDs have been identified before.[10,23] The authors measured hysteresis effects in current–voltage scans using MEH-PPV. Results were interpreted that deep traps with a concentration of ≈10^{16} cm^{-3} were responsible for hysteresis. By purification of the polymer, hysteresis-free currents were obtained. We purified our SY material via a number of subsequent precipitations, as described for MEH-PPV,[23] but observed no difference in hysteresis between unpurified and purified material (Note S4, Supporting Information). Therefore, our situation is different and the chemical nature of the different traps in SY does not originate from the presence of low-molecular-weight polymer fractions in the material or from trivial impurities that are soluble in common organic solvents.

We discuss the long recovery trends after relaxation observed for the intermediate and deep traps. We exclude that permanently present and active trap states in the material act as the deep electron traps and ascribe this unusual phenomenon to the fact that detrapping effectively deactivates the trap, followed by slow trap reactivation. The often-made differentiation of active traps states that are related to intrinsic defects (such as kinks in the polymer backbone) or that have an extrinsic origin (such as impurities remaining from the synthesis) is not

 © 2022 The Authors. Advanced Functional Materials published by Wiley-VCH GmbH

relevant in this regard. This is because our presumption is that charge trapping is fast for any trap site (intrinsic or extrinsic) that is present and accessible at switch-on. Also, there is no reason to assume that the charge trapping time for active trap sites is related to the energetic depth of the trap. Furthermore, we found that detrapping is much faster than trapping, and that the trapping time correlates with the length of the previous break time.

One explanation for slow charge trapping relates to permanently present, but difficult-to-access traps that are located at remote sites in the bulk of the polymer. In this case, trapping and detrapping is slow for morphological reasons. There are several arguments against such a scenario. First, if remote traps were permanently present in the material, it is not clear why detrapping is much faster than trapping, as observed. Second, we calculated the trap depths of ≈0.5 and 0.7 eV by assuming thermal emission out of the trap. For remote traps, the trap depth would in reality be much lower, because the measured detrapping time is then determined by the probability that an isolated trap becomes accessible and detrapping occurs. However, by systematically varying the electron affinity for a variety of polymers and by using chemical n-type doping,[2] it has clearly been shown that there exists a general impurity acting as the electron trap with an electron affinity ≈3.6 eV. For SY with an energy of the LUMO of 2.9 eV,[24] this indeed means that a trap with an actual trap depth of ≈0.7 eV does exist.

Therefore, we speculate that detrapping of the universal electron traps results in immediate trap deactivation. The chemical trap species remain present in the material and are accessible; however, the probability for trap reactivation and charge trapping at switch-on is low. This peculiar trap behavior provides important information on the chemical nature of the deep electron traps. For example, it has been observed that aggregates in MEH-PPV act as (shallow) charge traps and recombination centers.[25] Likewise, it has been proposed that carbonyl-containing end-groups in the polymer structure can be reduced electrochemically via reaction with the injected electrons and thus act as deep traps.[23] We argue that such trap species would not show the phenomenon of deactivation upon detrapping: for example, if the electron detraps from the carbonyl group at rest, it can immediately be reduced again at switch-on.

As a common origin for the omnipresent electron charge traps in conjugated polymers, oxygen, water, and hydrated oxygen complexes have been identified as likely candidates.[4,26–28] Not overselling the discussion, we mention findings in favor of the idea that hydrated oxygen complexes indeed act as charge traps, but that their probability of formation is effectively low. First, it has been reported that the neutral $H_2O \cdot O_2$ complex is very weakly bound, with a calculated binding energy of 0.016 eV[29] that is lower than the thermal energy. Therefore, oxygen and water (cluster) molecules are permanently present in the polymer, but usually not in the form of hydrated oxygen complexes that can immediately be reduced. The trap is stable once it has captured an electron, because the reduced $H_2O \cdot O_2^-$ species is an ion-dipole complex with a binding energy of 0.88 eV for dissociation to H_2O and O_2^-.[29] Support for a weakly bound neutral complex comes from the observation that the trap reactivation time strongly depends on the break time. If the oxygen and water molecules were mostly in the unbound state but remained in close proximity, we expect that the probability that a passing charge encounters now and then a water oxygen complex does not depend on the break time. Rather, the trap recovery trend suggests that after detrapping oxygen and water separate via diffusion, and the probability for an encounter and complex formation decreases with increasing time at rest. During device operation, trapped electrons recombine with free holes. This also results in trap deactivation, but the outcome is different from the situation at rest. Shortly after detrapping, water and oxygen are still close and in a dynamic equilibrium with the complex, which can immediately capture a free electron and stabilize again.

4. Conclusions

We studied the dynamics of electron trap filling and detrapping in SY PLEDs. For this purpose, we measured the device response to electrical driving and breaks covering the timescale from microseconds to hours. By measuring the performance decay after switch-on and the detrapping time after switch-off, we obtained information about the trap filling time and trap concentration, as well as the trap depth. From this analysis, we could identify the universal deep electron traps clearly. Surprisingly, trap filling of these deep traps proceeds over many minutes, clearly in contrast to the general notion that trap filling occurs on a timescale of a few hundreds of microseconds or less, irrespective of the depth of the trap level. We confirmed the slow trap filling process for P3HT and MEH-PPV PLEDs. Our observations are not consistent with the hypothesis that a permanently present and active chemical species in the material acts as the electron trap. Rather, it favors the proposed hydrated oxygen complex as the origin for the charge trap. Results suggest that the reduced (trapped) complex is stable, but that after detrapping oxygen and water separate via diffusion because the neutral complex is weakly bound. A slow diffusion process involved in the complex formation is in agreement with the slow trap filling observed. Our results on the surprisingly slow trap filling of the universal electron traps in semiconducting polymers are useful to pinpoint the chemical nature of the traps in further experimental and quantum-chemical studies.

5. Experimental Section

Dried (24 h, 0.1 mbar, 40 °C) SY (Merck) was dissolved in a concentration of 5 mg mL^{-1} in anhydrous THF or toluene, respectively. Solutions were stirred for 24 h at 60 °C before coating. Patterned ITO substrates (≈11 Ohms square^{-1}) were cleaned successively in acetone, ethanol, a 2 vol% aqueous solution of Hellmanex and deionized water using an ultrasonic bath. 40 nm thick PEDOT:PSS (HTL Solar, Ossila) films were spin-coated (1000 rpm s^{-1}, 60 s at 3000 rpm) from filtered (pore size 0.45 µm) solution and were then dried for 20 min at 120 °C. SY films with a thickness of (80 ± 10 nm) were coated inside a glove box (H_2O < 1 ppm, O_2 < 20 ppm). Before spin coating, solutions were stirred at room temperature for 20 min. Films were coated from unfiltered solutions for 60 s at 2000 rpm and 2000 rpm s^{-1}, and were then dried at 60 °C for 1 h inside the glove box. Calcium (10 nm) and aluminum (70 nm) were thermally evaporated through a shadow mask defining eight cells with an active area of 3.1 or 7.1 mm^2 per substrate.

© 2022 The Authors. Advanced Functional Materials published by Wiley-VCH GmbH

For the electron-only device, the PEDOT:PSS layer on ITO was replaced by a 20 nm thick aluminum layer. MEH-PPV (Sigma–Aldrich) and P3HT (regioregular, Sigma–Aldrich) were used as received and PLEDs were fabricated as described for SY. For P3HT, toluene (5 mg mL^{-1}) was used as the solvent. The low driving voltage for the P3HT PLED in Figure 3a is in agreement with literature.[30] For MEH-PPV, chlorobenzene (10 mg mL^{-1}) was used as the solvent.

For luminance measurements, devices were placed in an airtight holder and were measured under nitrogen atmosphere outside the glove box at room temperature using a factory-calibrated Konica Minolta LS-110 luminance meter with a close-up lens 110. The reflection loss of the top cover glass of the holder was not considered. Hysteresis, current, and light intensity transients were measured on the Paios measurement system (Fluxim AG, Switzerland). The light intensity was measured with a photodiode as photovoltage. The relationship between the measured photovoltage and the corresponding radiance/luminance is explained in the Supporting Information of reference.[31] Impedance measurements were carried out at 0 V on a Metrohm Autolab.

Optical and electrical simulations were performed with Setfos 5.1 (Fluxim AG, Switzerland). Simulation procedures and parameters are described in the Supporting Information Note S1. Optical constants of SY were taken from reference[32] and were confirmed by simulation of experimental transmission spectra measured previously.[33] Photoluminescence spectra were measured on a Horiba Jobin Yvon Fluorolog spectrometer.

Supporting Information

Supporting Information is available from the Wiley Online Library or from the author.

Acknowledgements

Financial support from the Swiss National Science Foundation (grant IZBRZ2_186261 and P500PT_203221) is acknowledged.

Open access funding provided by ETH-Bereich Forschungsanstalten.

Conflict of Interest

The authors declare no conflict of interest.

Data Availability Statement

The data that support the findings of this study are available in the supplementary material of this article.

Keywords

charge transport, charge trap dynamics, electron trap, polymer light emitting diodes, semiconducting polymers

Received: June 28, 2021
Revised: March 28, 2022
Published online:

[1] Q. Niu, R. Rohloff, G.-J. A. H. Wetzelaer, P. W. M. Blom, N. I. Crăciun, *Nat. Mater.* **2018**, *17*, 557.
[2] M. Kuik, G.-J. A. H. Wetzelaer, H. T. Nicolai, N. I. Craciun, D. M. De Leeuw, P. W. M. Blom, *Adv. Mater.* **2014**, *26*, 512.
[3] H. T. Nicolai, M. Kuik, G. A. H. Wetzelaer, B. de Boer, C. Campbell, C. Risko, J. L. Brédas, P. W. M. Blom, *Nat. Mater.* **2012**, *11*, 882.
[4] D. Abbaszadeh, A. Kunz, N. B. Kotadiya, A. Mondal, D. Andrienko, J. J. Michels, G.-J. A. H. Wetzelaer, P. W. M. Blom, *Chem. Mater.* **2019**, *31*, 6380.
[5] Q. Niu, G.-J. A. H. Wetzelaer, P. W. M. Blom, N. I. Crăciun, *Adv. Electron. Mater.* **2016**, *2*, 1600103.
[6] N. B. Kotadiya, A. Mondal, P. W. M. Blom, D. Andrienko, G.-J. H. A. Wetzelaer, *Nat. Mater.* **2019**, *18*, 1182.
[7] Q. Niu, G.-J. A. H. Wetzelaer, P. W. M. Blom, N. I. Crăciun, *Appl. Phys. Lett.* **2019**, *114*, 163301.
[8] I. Rörich, Q. Niu, B. van der Zee, E. del Pino Rosendo, N. I. Crăciun, C. Ramanan, P. W. M. Blom, *Adv. Electron. Mater.* **2020**, 1700643.
[9] M. Kuik, L. J. A. Koster, A. G. Dijkstra, G. A. H. Wetzelaer, P. W. M. Blom, *Org. Electronics* **2012**, *13*, 969.
[10] D. Abbaszadeh, A. Kunz, G. A. H. Wetzelaer, J. J. Michels, N. I. Crăciun, K. Koynov, I. Lieberwirth, P. W. M. Blom, *Nat. Mater.* **2016**, *15*, 628.
[11] S. Burns, J. MacLeod, T. T. Do, P. Sonar, S. D. Yambem, *Sci. Rep.* **2017**, *7*, 40805.
[12] S. Tang, L. Edman, *J. Phys. Chem. Lett.* **2010**, *1*, 2727.
[13] W. Shockley, W. T. ReadJr, *Phys. Rev.* **1952**, *87*, 835.
[14] T. Yamada, D. Zou, H. Jeong, Y. Akaki, T. Tsutsui, *Syn. Metals* **2000**, *111*, 237.
[15] Z. D. Popovic, H. Aziz, *IEEE J. selected topics quantum electronics* **2002**, *8*, 362.
[16] M. Yahiro, D. Zou, T. Tsutsui, *Syn. Metals* **2000**, *111*, 245.
[17] D. Zou, M. Yahiro, T. Tsutsui, *Jpn. J. Appl. Phys.* **1998**, *37*, L1406.
[18] D. Zou, M. Yahiro, T. Tsutsui, *Appl. Phys. Lett.* **1998**, *72*, 2484.
[19] A. J. A. B. Seeley, R. H. Friend, J.-S. Kim, J. H. Burroughes, *J. Appl. Phys.* **2004**, *96*, 7643.
[20] K. S. Rao, Y. N. Mohapatra, *J. Luminescence* **2014**, *145*, 793.
[21] L. Lepnev, A. Vaschenko, A. Vitukhnovsky, S. Eliseeva, O. Kotova, N. Kuzmina, *Syn. Metals* **2009**, *159*, 625.
[22] M. M. Mandoc, B. de Boer, G. Paasch, P. W. M. Blom, *Phys. Rev. B.* **2007**, *75*, 193202.
[23] N. I. Craciun, Y. Zhang, A. Palmaerts, H. T. Nicolai, M. Kuik, R. J. P. Kist, G. A. H. Wetzelaer, J. Wildeman, J. Vandenbergh, L. Lutsen, D. Vanderzande, P. W. M. Blom, *J. Appl. Phys.* **2010**, *107*, 124504.
[24] J. Xu, A. Sandström, E. M. Lindh, W. Yang, S. Tang, L. Edman, *ACS Appl. Mater.* **2018**, *10*, 33380.
[25] H.-E. Tseng, C.-Y. Liu, S.-A. Chen, *Appl. Phys. Lett.* **2006**, *89*, 233510.
[26] J.-M. Zhuo, L.-H. Zhao, R.-Q. Png, L.-Y. Wong, P.-J. Chia, J.-C. Tang, S. Sivaramakrishnan, M. Zhou, E. C.-W. Ou, S.-J. Chua, W.-S. Sim, L.-L. Chua, P. K.-H. Ho, *Adv. Mater.* **2009**, *21*, 4747.
[27] H.-E. Tseng, K.-Y. Peng, S.-A. Chen, *Appl. Phys. Lett.* **2003**, *82*, 4086.
[28] V. Kažukauskas, H. Tzeng, S. A. Chen, *Appl. Phys. Lett.* **2002**, *80*, 2017.
[29] A. J. Bell, T. G. Wright, *Phys. Chem. Chem. Phys.* **2004**, *6*, 4385.
[30] G. Yu, H. Nishino, A. J. Heeger, T.-A. Chen, R. D. Rieke, *Syn. Metals* **1995**, *72*, 249.
[31] M. Diethelm, A. Schiller, M. Kawecki, A. Devižis, B. Blülle, S. Jenatsch, E. Knapp, Q. Grossmann, B. Ruhstaller, F. Nüesch, R. Hany, *Adv. Funct. Mater.* **2020**, *30*, 1906803.
[32] T. Lanz, E. M. Lindh, L. Edman, *J. Mater. Chem. C* **2017**, *5*, 4706.
[33] M. Diethelm, Q. Grossmann, A. Schiller, E. Knapp, S. Jenatsch, M. Kawecki, F. Nüesch, R. Hany, *Adv. Opt. Mater.* **2019**, *7*, 1801278.

© 2022 The Authors. Advanced Functional Materials published by Wiley-VCH GmbH